



“Gheorghe Asachi” Technical University of Iasi, Romania



MONITORING AND ASSESSMENT OF MINING SUBSIDENCE IN A METAL MINE IN CHINA

Haijun Zhao*, Fengshan Ma, Yamin Zhang, Jie Guo

Chinese Academy of Sciences, Institute of Geology and Geophysics, Key Laboratory of Engineering Geomechanics,
100029 Beijing, China

Abstract

The occurrence of ground subsidence induced by backfill mining method becomes a new threat to many mines. The current paper presents a typical example in the Jinchuan mine in China. Based on actual situations of mining subsidence and damage, GPS monitoring networks were successively established in three neighboring mine fields in the Jinchuan mine at the beginning of 2001. An integrated monitoring network composed of 848 monitoring points to study mining subsidence was eventually set up in the entire mining area in the first half of 2005. Based on combined field investigation and monitoring, it revealed the characteristics of mining subsidence in the Jinchuan mine. In addition, the mining subsidence mechanisms, comparison between the monitoring results and the ground subsidence, correlations with the damage of underground facilities and the extracted ore tonnage were discussed. Furthermore, several countermeasures were proposed according to the mining subsidence and damage situations.

Key words: assessment, backfill mining, ground subsidence, monitoring

Received: December, 2011; *Revised final:* July, 2012; *Accepted:* July, 2012

1. Introduction

Ground subsidence is a common engineering geological problem in underground mining. So far, many studies have been conducted on this subject. However, previous investigations mainly focused on mining subsidence induced by long-wall or room-and-pillar mining methods (Cui et al., 2001; Sheorey et al., 2000; Singh and Singh, 1998). Very few studies have been conducted on ground subsidence induced by the advanced backfill mining method (Donovan and Karfakis, 2001; Yamaguchi and Yamatomi, 1985) mainly because the advantages of backfill mining have been overestimated (Cowling, 1998; Liu et al., 1998). The backfill mining method was commonly believed to effectively control the ground pressure and prevent possible ground subsidence and cracks from occurring (Bell et al., 2000; Swift and Reddish, 2002; Singh and Saxena,

1991), but the outcome did seem to overthrow this belief. Large-scale ground subsidence and damage also can be induced by backfill mining, thus resulting in severe damage to buildings, roads, shafts, and other facilities (Oyler et al., 2001; Peng, 1992). In the current paper, the Jinchuan mine was studied because it presents a prime example of ground subsidence triggered by backfill mining.

The Jinchuan mine is the largest nickel deposit in China. Its proven nickel reserve ranks the first in China and the third in the world. The mining area is approximately 6.5 km long, tens to hundreds of meters wide, and extends to more than 1,000 m deep (Fig. 1). The strike of the main ore body is northwest and dips to the southwest, and the dip angle is range from 40° to 70°. The mining area strata are Precambrian mesometamorphic rocks, and the stratum lithology is principally composed of banded migmatite, marble, amphibolite, ultrabasic rocks,

* Author to whom all correspondence should be addressed: e-mail: zhaohaijun@mail.iggcas.ac.cn; zhaohj04@mails.gucas.ac.cn; Phone: +86-13661238100; Fax:+86-10-82998590

diabase, micaceous quartzite, and sandstone. The ore-bearing ultrabasic rocks intruded into the Precambrian strata and were divided into four mine fields due to the partition of the faults in the mining area. At present, mine field Nos. 1, 2, and 3 are being exploited, whereas mine No. 4 remains undeveloped. In the Jinchuan mine, different sizes of faults, joints, and contact fracture zones that intersect with one another are well-developed. The maximum principal stress is horizontal and oriented northeast–southwest, which is perpendicular to the strike of the ore body, showing high magnitude of stress. The principal stresses gradually increase with depth. For instance, the maximum principal stress reaches 45 MPa at the depth of 500 m.

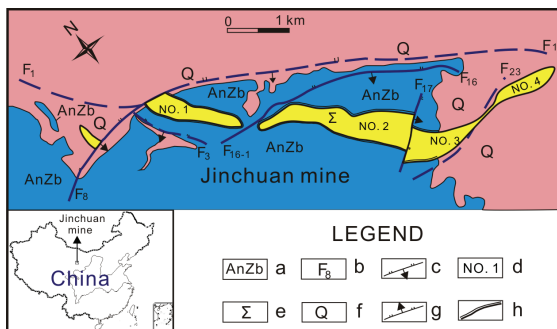


Fig. 1. Location and geological map of the Jinchuan mine.

(a) Metamorphic rocks of lower Proterozoic, (b) fault number, (c) reverse fault, (d) mining area number, (e) ore-bearing ultrabasic rocks, (f) Quaternary, (g) normal fault, (h) contact zone

Mine field No. 1 is a large-scale open-pit mine completely converted to an underground mine in 1990 after about 30 years of open-pit mining. The open pit is approximately 1,300 m long, 670 m wide, and 200–310 m deep. Advanced backfill mining method was employed in mine No. 1 to ensure the safety of the stope roofs and pit slope stability because of high *in-situ* stresses, fractured rock masses, and poor massif stabilities in the mining area. Nevertheless, striking ground subsidence and damage occurred after the transition from open-pit to underground mining. The pit slope showed different degrees of deformation and damage, and a large number of ground fissures were generated in and around the open pit.

Mine field No. 2 is the main mining area in the Jinchuan mine. The nickel mineral resource accounts for 75.2% of the total reserves of the Jinchuan mine. Mine field No. 2 contains 351 ore bodies, where ore body Nos. 1 and 2 account for 99.3% of the total reserves. Ore body No. 1 is the main ore body mined in mine No. 2 and is 1,600 m long, 100 m wide, and extends from 350 m below the surface to more than 1,000 m. Since 1990, simultaneous backfill mining in the 1,250 and 1,150 m sublevels has been implemented to increase ore production. However, evident ground subsidence and ground fissures appeared at the end of 1999. Since then, the issue of backfill mining-induced ground

subsidence and damage has received increasing attention. By the end of 2010, the mining area was enlarged to about 100,000 m², and the volume of the filling body cumulated to approximately 10 million m³. Thus, mine No. 2 experienced the worst effects of mining subsidence and damage in the Jinchuan mine.

Mine No. 3 is a newly exploited mine field after 2004. Although the potential hazard of mining subsidence was taken into account in the infrastructure construction, the range of influence was seriously underestimated at that time. Therefore, deformation and damage of buildings and structures have prominently increased with the rapid increase of underground mining in recent years.

In summary, the Jinchuan nickel mine is a large mine consisting of several neighboring mine fields. Although some differences in the mine-field exploitation histories and mining conditions exist, they are exposed to the same threat, i.e., large-scale ground subsidence induced by backfill mining. Since 2001, GPS monitoring system has been established in these mine fields successively to study the characteristics and regularities of mining subsidence. Eventually, a complete GPS monitoring network, capable of covering the entire mining area, was set up in the first half of 2005. Continuous field monitoring was conducted from June 2001 to 2010, and large amounts of data were obtained. The current study presents the characteristics and regularities of the mining subsidence based on the duration of GPS monitoring and field investigations. In addition, the subsidence mechanisms, correlations with the damaged underground facilities and the extracted ore tonnage are also discussed. Through this research, a clear understanding of the ground subsidence induced by long-term backfill mining in the Jinchuan mine is achieved, which can be of great importance in the design of mines using the backfill mining method.

2. Deformation and damage of the ground surface and engineering works

In the Jinchuan mine, long-term underground backfill mining resulted in prominent ground subsidence and damage. Mining subsidence already caused serious deformation and damage to shafts, tunnels, buildings, and other engineering works in the seriously affected areas. In addition, more engineering works are in danger of being destroyed. Altogether, the following characteristics were recorded in the mining area.

(a) Ground surface deformation and damage: large-scale ground movement and ground fissures were triggered by underground mining. In mine No. 1, the pit wall underwent significant deformation and damage (Fig. 2a). The severely deformed and collapsed areas were mainly distributed in the southeastern part of the open pit. Overall, toppling failure was the most typical feature in the open pit. As a result, some benches severely collapsed, and a

series of parallel ground fissures and counter-inclined scarps occurred on the surface. Unfortunately, the range and extent of the pit wall deformation and failure have also significantly increased with the rapid increase of the underground mining in recent years. In particular, in mine No. 2, approximately 40 large ground fissures had formed on the surface since 1999 (Fig. 2b). These ground fissures were mainly distributed in the upper surface of the ore body and roughly parallel to the strike of the ore body, showing scattered positions, unconnected distributions, and varied crack widths. Several large ground fissures were connected end to end, showing larger openings and extended lengths.

(b) Deformation and damage of surface buildings and structures: the Jinchuan mine is located in mountainous areas, thus few surface buildings and structures were built in the mining area. Nevertheless, some buildings and structures showed differential settlement and break within the subsidence areas (Fig. 3). At present, only a few irreplaceable buildings and structures still operate by applying continuous reinforcement measures. Most of the buildings and structures that showed serious deformation and damage were abandoned or relocated. Further, some concrete roads and drainage channels were ruptured due to uneven settlement of

the ground surface. These phenomena greatly affected normal operation.

(c) Deformation and damage of sinking and driving engineering: large-scale mining subsidence and deformation frequently cause deformation and rupture to the shafts and tunnels (Fig. 4). For example, in mine No. 1, several exploratory shafts located at the pit bottom were destroyed and forcibly abandoned. In mine No. 2, the mining-induced rock mass movement caused serious damage to a ventilation shaft in 2005. The shaft was destroyed and filled with collapsed rock fragments. Only the upper segment of the shaft from the ground surface to a depth of 170 m remained undamaged and can be seen directly. In addition, the deformation and damage of tunnels were also prominent. The convergence displacement of the surrounding rocks was from a few centimeters to dozens of centimeters. In addition, the deformation and damage of tunnels showed evident stage characteristics. Initial deformation usually lasts roughly 30 days, and the maximum displacement can reach 6 mm per day. Long-term creep deformation usually takes several months or even years after excavation. However, some tunnels excavated inside or close to the ore body are always deformed because of continuous disturbances from mining activities.

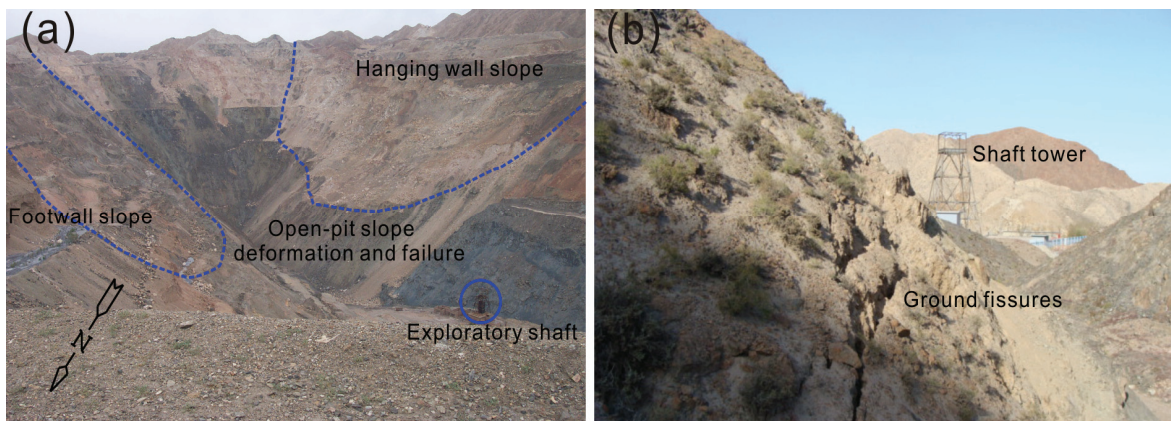


Fig. 2. Pictures of the ground surface deformation and damage. (a) Open-pit slope deformation and failure in mine No. 1, (b) ground fissure in mine No. 2

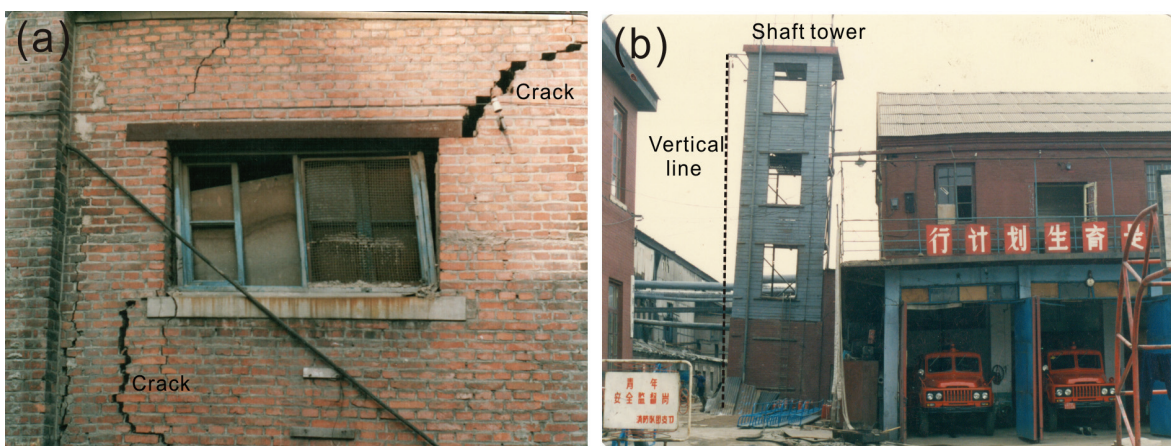


Fig. 3. Pictures of the deformed and damaged buildings and structures. (a) Deformation and break of a house, (b) inclination of a shaft tower

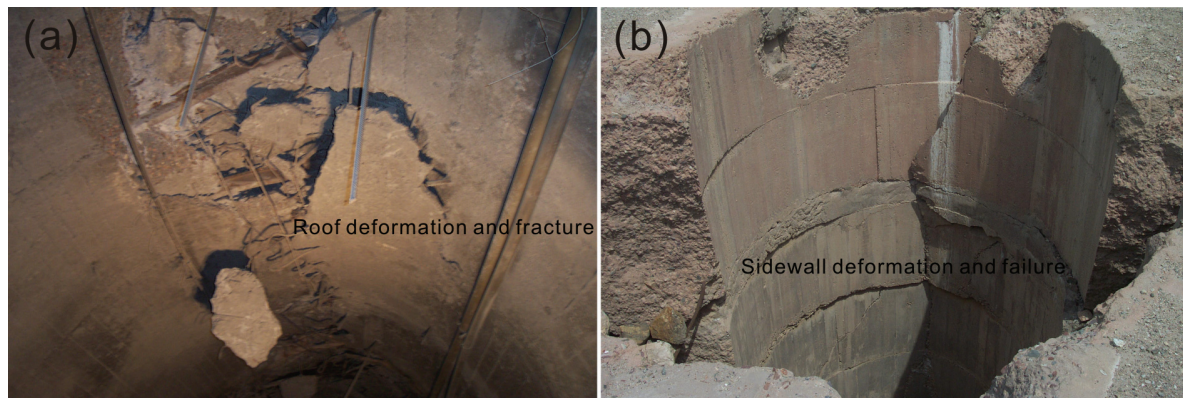


Fig. 4. Pictures of the deformed and damaged sinking and driving engineering. (a) Deformation and damage of a tunnel, (b) deformation and damage of a shaft

3. Methodology

3.1. GPS monitoring of ground subsidence

At present, several methods for predicting the magnitude of mining-induced subsidence with reasonable degree of accuracy and precision are widely used. Such techniques include geodetic measurements and GPS techniques (Guéguen et al., 2009), synthetic aperture radar techniques (Carnec and Delacourt, 2000), and many other traditional measurements (e.g., total station, level, and surveying robot). Each of these methods has its special characteristics and relative adaptability (Chrzanowski et al., 1989; González-Nicieza et al., 2005). However, their common objective is to estimate the likelihood and magnitude of ground subsidence induced by the extraction of underground mineral resources.

In the current study, the GPS technique was adopted to monitor ground subsidence because of the high-precision requirement in the mining area. GPS monitoring is characterized by ease of operation, high precision and efficiency, as well as large-scale and real-time synchronous measurements of vertical and horizontal displacements. In addition, GPS measurements are immune to the effects of surface relief and climatic changes. Therefore, this method is adaptable to almost all regions with a wide field of view from the top. In recent years, the GPS technique has been extensively used in various measuring works, such as in surveying of global plate movements and earthquakes (Shi et al., 2010), large-scale ground subsidence (Baldi et al., 2009), landslides (Peyret et al., 2008), stability of buildings and infrastructural facilities (Shimizu et al., 2006), and mines (Chrzanowski et al., 2000; Lü et al., 2008).

3.2. Monitoring design and application

The GPS monitoring technology was first applied to mine No. 2 in 2001 because it had the largest output and, especially, the most prominent ground subsidence and damage. The monitoring

network is composed of a reference net and a deformation monitoring net on the surface of the mining area. The reference net contains seven datum marks, which were all built on firm bedrocks and away from the influence of underground mining and other disturbance sources. Thus far, inspection results have shown that the reference net is stable and reliable.

In mine No. 2, 101 GPS measuring points were established in 2001 to set up the initial deformation monitoring network. These points were mainly laid out along the exploratory lines in the mining area. Further, an additional monitoring line was laid out on the upper surface of the ore body, perpendicular to the exploratory line. Later, in 2003, GPS monitoring technology was employed in mine No. 1. At that time, 122 GPS monitoring points were established. Similarly, these points were laid out along the exploratory lines in the mining area. However, the initial monitoring ranges did not meet the requirements because of the expansion of the depressed areas. Thus, many new monitoring points were added to mine Nos. 1 and 2 in the first half of 2005 during the establishment of the initial monitoring network in mine No. 3. Thus, an integrated monitoring network that contained 848 monitoring points was eventually set up in the entire surface of the Jinchuan mine to study the mining subsidence (Fig. 5). So far, to the authors' knowledge, it is the largest GPS monitoring network for studying mining-induced ground subsidence in the world.

The Z-12-type GPS receiver and antenna apparatus (Ashtech, USA) were employed in the monitoring. The nominal accuracy of the horizontal displacement was $3 \text{ mm} + 0.5 \text{ ppm}$, and the nominal accuracy of the vertical displacement was $5 \text{ mm} + 1 \text{ ppm}$. For practical applications, four suits of GPS with static model were used for simultaneous monitoring. The measurement time for each segment lasted 1 to 2 hours, and the data-collection interval was 10 seconds. The data processing results showed that the precision of the monitored data was higher than expected because the mean square error of the points was about $\pm 1.96 \text{ mm}$ in the previous

monitoring. By the end of 2010, field monitoring had been carried out biannually for 10 years in mine No. 2, 7 years in mine No. 1, and 5 years in mine No. 3 (Fig. 6).

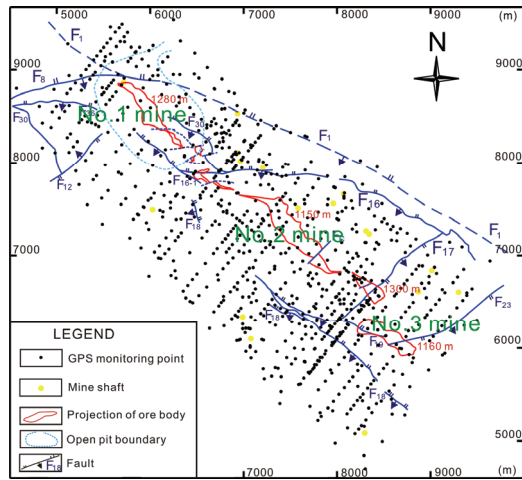


Fig. 5. Distribution of GPS monitoring points in the entire surface of the Jinchuan mine

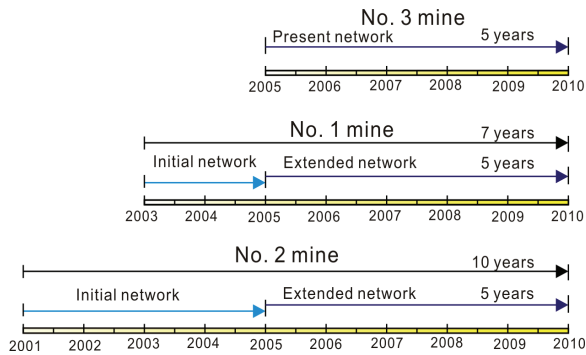


Fig. 6. Sketch illustrations of the establishment of the monitoring networks and cumulated times of monitoring in the three mine fields, respectively

4. Monitoring results

According to the large amount of monitored data, the displacement of each monitoring point was calculated for each measuring cycle based on baseline processing, constraint network adjustment, and coordinate conversion. The results showed that most of the monitoring points underwent changes, and three different subsidence troughs were formed in the three mine fields. The overall stereogram of the subsiding basin is shown in Fig. 7.

In mine No. 1, a complex subsidence trough centered on the underground mined-out space dramatically formed, characterized by pit slope subsidence and bottom uplift. In mine No. 2, a prominent subsidence trough centered on the underground mined-out space formed on the ground. In mine No. 3, the subsidence trough was similar to that of mine No. 2, although it was yet small at this stage. In the seriously affected areas of the three mine fields, the annual settlement increased significantly.

Overall, the primary characteristics of the mining subsidence in the three mine fields are summarized next.

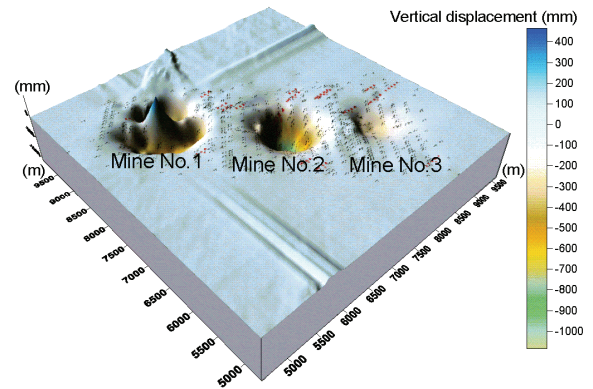


Fig. 7. Overall stereogram of subsiding basin in December 2010. Reference measure: June 2005

4.1. Ground subsidence in mine No. 1

Striking ground subsidence in mine No. 1 occurred after the transition from open-pit to underground mining. The most important feature was that evident bottom uplift occurred under the influence of underground mining and the compression of the overlying pit slope. As shown in Figs. 8a and b, two subsiding centers were developed in the hanging wall and the footwall surface of the ore body, respectively. The upheaval center was located at the center of the pit bottom. Several monitoring points at the pit bottom had successively shown rising trend during the past eight years.

The subsidence area obviously expanded far away from the pit outline at the hanging wall surface, whereas it was basically around the pit boundary at the footwall surface with the expansion of underground mining, as shown in the comparison between Figs. 8a and b. Since June 2003, the maximum cumulated subsidence had reached 767 mm at the hanging wall surface of the open pit. In contrast, the maximum cumulated subsidence had reached 1,078 mm at the footwall surface of the open pit. In addition, the upheaval area was located between exploration lines 22 and 28. The maximum bottom uplift had reached 684 mm by the end of 2010.

In the open pit, the bottom uplift is directly related to the increase of horizontal stresses in the rock mass sandwiched between the pit bottom and the top of the filling body. Hence, a plane strain model is assumed for the convenience of discussion (Fig. 9). The upper part of the pit bottom can be considered as thinly bedded panel parallel to the ground surface. With the increase in mining depth, the sizes of both sides of the filling body and the convergence displacements of the filling body are inevitably increased. However, the scale of the bedded panel is almost unchanged during mining.

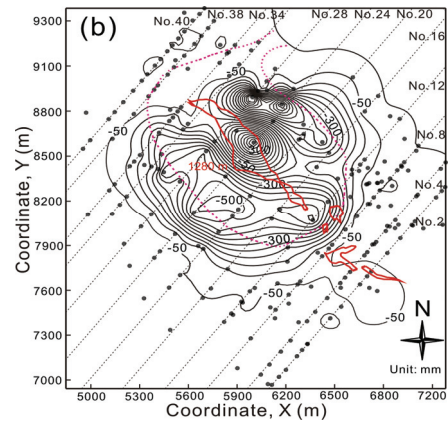
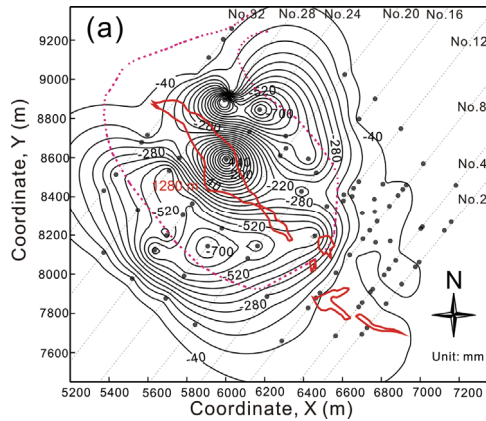


Fig. 8. Contour maps of vertical displacements in December 2010 in mine No. 1. (a) Reference measure: June 2003, (b) reference measure: June 2005

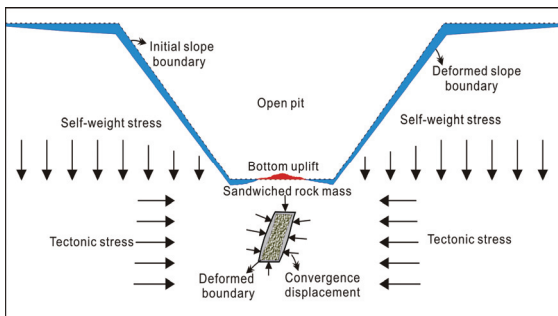


Fig. 9. Schematic illustration to demonstrate the deformation of the open pit bottom

Besides, the lateral bracing forces on both sides of the bedded panel are progressively increased under the effects of the dead weight of the pit slope and the high-level of the tectonic stress. As a result, horizontal stress in the bedded panel is greatly enhanced and which caused the uplift of the pit bottom.

In terms of horizontal displacements, a remarkable active region that took the ore body as the center formed on the ground surface (Figs. 10a and b). The magnitudes of cumulative horizontal displacements were particularly striking in the high segment of the pit slope and decreased greatly from the boundaries of the open pit. The severely influenced area was situated between exploratory lines 16 and 28. The horizontal displacements were obviously larger at the hanging wall surface than at the footwall surface of the ore body. Overall, the magnitudes of horizontal displacements at the hanging wall surface were generally 2 to 3 times larger than those at the footwall surface. As shown in the comparison between Figs. 10a and b, the planimetric active region obviously expanded far away from the pit outline.

Similarly, the range and magnitude of the expanded area were larger at the hanging wall surface than at the footwall surface. By the end of 2010, the maximum cumulated horizontal displacement had reached 1,407 mm at the hanging wall surface. The maximum cumulated horizontal displacement had reached 1,543 mm at the footwall surface.

4.2. Ground subsidence in mine No. 2

In mine No. 2, 10 years of monitoring provided large amount of monitoring data. The calculated results quantitatively described the features of the mining subsidence in the mining area.

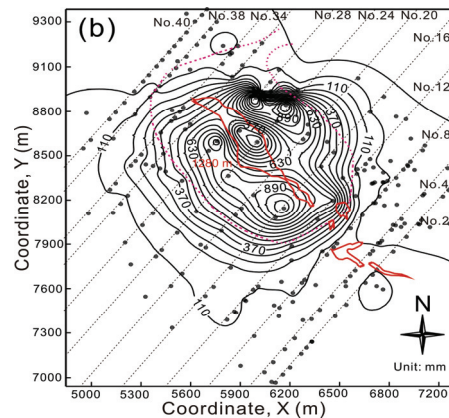
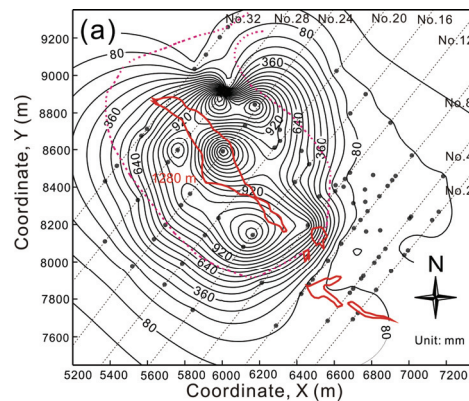


Fig. 10. Contour maps of horizontal displacements in December 2010 in mine No. 1. (a) Reference measure: June 2003, (b) reference measure: June 2005

The results showed that most of the monitoring points have changed. A large-scale subsidence trough progressively developed and expanded with the increase of the mining depth. As shown in Figs. 11a and b, the subsidence trough has an overall oval shape. The extent of the ground subsidence is obviously larger at the hanging wall

than that at the footwall. The subsidence areas with large positive curvatures on both sides of the subsiding center were exactly the same places where the two fissure zones were located.

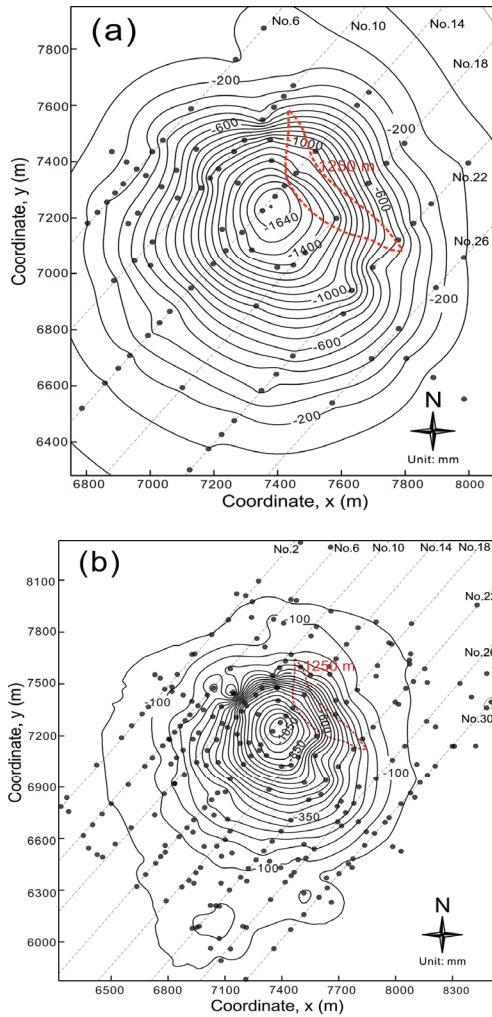


Fig. 11. Contour maps of vertical displacements in December 2010 in mine No. 2. (a) Reference measure: June 2001, (b) reference measure: June 2005

The subsidence trough extended 2.3 km along the exploratory line and 1.5 km along the strike of the ore body. The subsiding center was seated at monitoring point 14-4, which was 340 m away from line No. 14 shaft and 130 m away from the projection of the ore body (sublevel 1,250 m) at the surface. The maximum subsidence at the subsiding center increased prominently with the increase in mining depth during the past 10 years. By the end of 2010, the maximum vertical displacement had reached 1,720 mm. In terms of horizontal displacements, a remarkable planimetric active region was developed on the ground surface, as shown in Figs. 12a and b. The prominent horizontal displacements were distributed between exploratory lines 10 and 18.

In the measuring line No. 14, which was perpendicular to the strike of the ore body, the monitoring point 14-9 kept the maximum horizontal displacement. The horizontal displacements at the

hanging wall surface were larger than those at the footwall surface of the ore body. Besides, the greater the horizontal displacements were, the closer the monitoring point to the vertical projection of the ore body. By the end of 2010, the maximum cumulated horizontal displacement had reached 1,135 mm (Fig. 12a). Similarly, as shown in the comparison between Figs. 12a and b, the range and magnitude of the expanded area were larger at the hanging wall surface than at the footwall surface over the last five years.

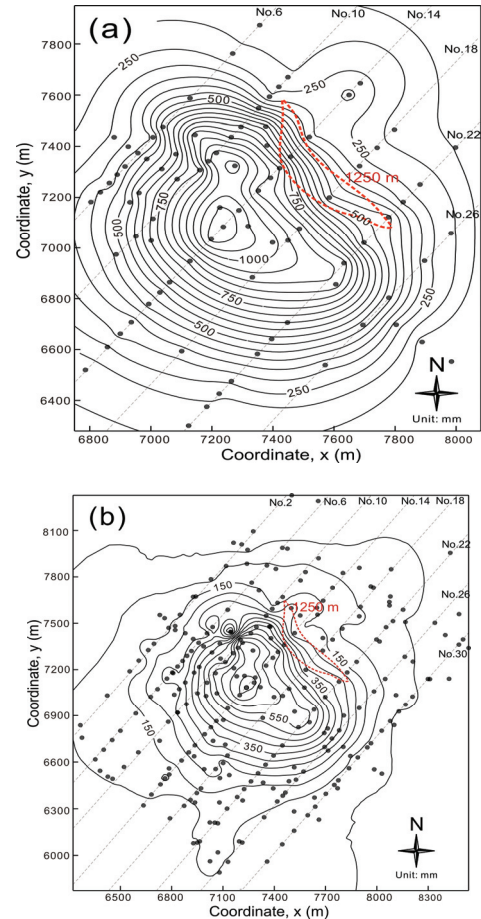


Fig. 12. Contour maps of horizontal displacements in December 2010 in mine No. 2. (a) Reference measure: June 2001, (b) reference measure: June 2005

4.3. Ground subsidence in mine No. 3

As shown in Figs. 13 and 14, a small round-shaped surface depression was formed on the surface of mine No. 3. The severely influenced area was situated between exploratory lines 38 and 46. The subsiding center was located at the monitoring point 42-12. By the end of 2011, the maximum cumulated vertical displacement had reached 316 mm and the maximum horizontal displacement had reached 158 mm. In addition, few ground fissures were observed in this mine field. Overall, the range and magnitude of the subsiding basin were small compared with the mine No. 2 because of its short exploration history and relative small mining capacity. Thus, the ground subsidence was at the early stage of development.

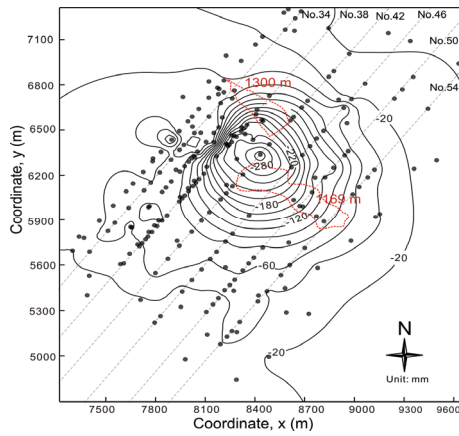


Fig. 13. Contour maps of vertical displacements in December 2010 in mine No. 3. Reference measure: June 2005

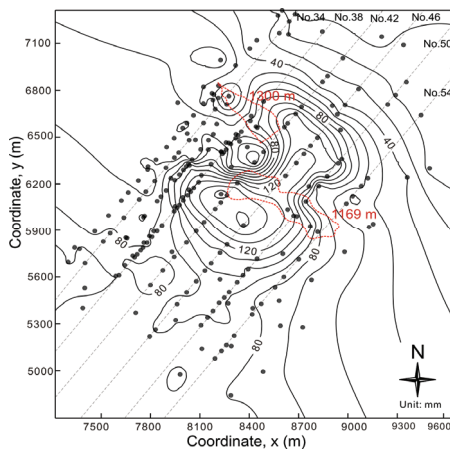


Fig. 14. Contour maps of horizontal displacements in December 2010 in mine No. 3. Reference measure: June 2005

5. Discussion

5.1. Mining subsidence mechanisms

In the current work, the occurrence of mining subsidence and damage proved that large-scale rock mass movement cannot be avoided absolutely despite the application of advanced backfill mining method. The misconception that the backfill mining method can effectively prevent evident ground subsidence and cracks from occurring lies in the inaccurate understanding of the mining and filling process. At any rate, backfill mining cannot be simply regarded as rapid replacement of the ore body with filling compound. In general, an access way usually takes about a week to be mined, and the preparatory work of backfilling the excavated access takes about two weeks. Thus, a cycle of mining and filling an access way takes about three weeks.

Additionally, the filling compound must still undergo a gradual solidification and hardening process after filling the mined-out space, and the final Young's modulus of the filling bodies is one to two orders of magnitude smaller than that of the ore body. Therefore, if mining and filling is considered

as a rapid replacement process, the substantial movement and elastic-plastic deformation of the surrounding rocks might be neglected. These movement and deformation behaviors of the surrounding rocks in the hanging wall and footwall of the mined-out space play an important role in ground subsidence.

On the other hand, the large-scale adjustment and redistribution of the stress field and the reduction of the deformation modulus of the surrounding rocks are bound to occur under the influence of repeated mining activities. In addition, a large amount of unfilled mine goaf provides a large space for the movement and deformation of the surrounding rocks. In the mine, approximately 5% of the mined-out space cannot be eventually backfilled, including some blind shafts, haulage drifts, underground warehouses, equipment houses, and control rooms. Furthermore, the mined-out space is not completely backfilled. In general, about 10–30 cm void spaces exist between the filling bodies and the stope roofs. Therefore, the surrounding rocks of the backfilled and unfilled spaces inevitably moved and deformed under conditions of high horizontal geo-stress and extremely fractured rock mass. Consequently, movement and deformation of the rock mass surrounding the mined-out spaces are induced, eventually triggering ground subsidence and damage.

5.2. Comparison between the monitoring results and ground subsidence

In general, the monitoring results were consistent with the actual situations. From the settlement contour maps, the subsiding centers of the three mine fields were mainly distributed at the hanging wall surface of the ore body. In mine No. 1, underground mining brought about serious effects on the hanging wall slope, thus showing large deformed area and considerable displacement. In contrast, underground mining had relatively little effects on the footwall slope. Therefore, actual ground subsidence and ground fissures intensively developed in the hanging wall pit slope. In mine No. 2, the monitored ground subsidence and damage were very prominent because the mine had a long-term and large-scale mining history.

The most striking feature was that two subparallel fissure zones developed on the ground surface (Fig. 11). These ground fissures were mainly caused by the tension stresses of the ground deformation. Fissure zone No. 1 was distributed between exploratory lines 10 and 26. The strikes of these ground fissures varied from 32° northwest to the north with a length of approximately 1 km. In this zone, ground fissures were mainly developed in the contact zone between the ultrabasic rocks and the banded migmatite (Fig. 12). On the other hand, fissure zone No. 2 was distributed on the upper surface of the ore body between exploratory lines 8 and 28, approximately 500 m away from fissure zone No. 1. In this fissure zone, the overall strike of the

ground fissures was approximately 47° northwest with a length of more than 1 km. These ground fissures were mainly developed in the fracture zones of the banded migmatite and the penetrating dikes. In mine No. 3, the issue of ground subsidence and damage was not significant due to its short mining history and small ore output. Thus, the maximum settlement and the subsidence area were relatively small and agreed with the actual situations.

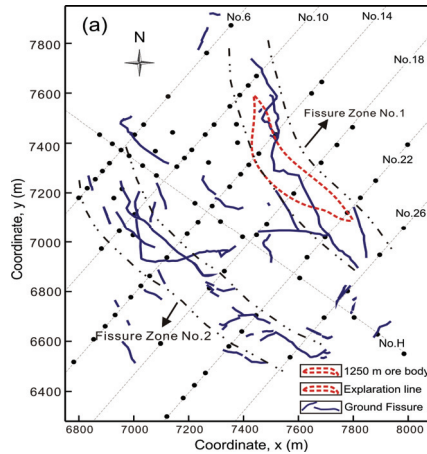


Fig. 11. The plane distribution of ground fissures in mine No. 2

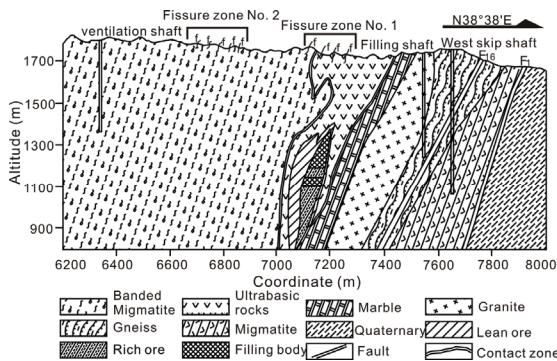


Fig. 12. The geological section along the exploratory line No. 19 in mine No. 2

5.3. Correlations between the ground subsidence and the damage of underground facilities

The survey found out that the position of the severely affected ground surface corresponded well with the damage of the underground sinking and driving engineering. As mentioned earlier, large-scale mining subsidence and deformation had caused obvious deformation and damage to tunnels and shafts. The most prominent feature was that the surface projections where the tunnels and shafts frequently showed deformation and damage were exactly located in the ground subsidence trough. For instance, in mine No. 2, the frequently and severely deformed and damaged tunnels were mainly distributed between exploratory lines 14 and 18, precisely coinciding with the location of the subsidence trough.

In these regions, maintenance and strengthening engineering works were significantly greater than elsewhere, resulting in great economic losses and production difficulties in the mine. Therefore, the current study offered positive contribution and guidance in determining support patterns of underground engineering works and in reducing the repair and production costs through comparative study of the ground subsidence with the damage to the underground engineering works.

5.4. Correlations between the ground subsidence and the extracted ore tonnage

The range and magnitude of the ground subsidence increased conspicuously with the increase of the annual extracted ore tonnage. In mine No. 1, the extracted ore tonnage was 1.32 million tons in 2003 and reached 1.82 million tons in 2010. Ore production increased 1.4 times from 2003 to 2010, whereas the corresponding maximum subsidence of the pit bottom increased 2.6 times from 109 mm to 278 mm. In mine No. 2, the extracted ore tonnage was 2.27 million tons in 2001 and reached 4.18 million tons in 2010. Ore production increased 1.8 times from 2001 to 2010, whereas the corresponding maximum subsidence increased 1.5 times from 149 mm to 217 mm. Similarly, in mine No. 3, the extracted ore tonnage was 0.4 million tons in 2005 and reached 1.3 million tons in 2010. Ore production increased 3.3 times from 2005 to 2010, whereas the corresponding maximum subsidence increased 1.2 times from 42 mm to 49 mm. In addition, as shown in the settlement contour maps, expansion of the subsidence areas were also prominent in the past few years.

5.5. Countermeasures for mining subsidence and damage

Reasonable production plan and engineering design are extremely important to reduce and prevent subsidence disasters. Although mining subsidence is a common phenomenon, it is a very dangerous sign for underground mining that employed the backfill mining method. Backfill mining method was believed to prevent evident ground subsidence; thus, various supporting facilities were built around and on the top surface of the ore bodies to save costs.

Under such conditions, mining subsidence poses a grave threat to the stability and safety of the engineering works. The Jinchuan mine is the typical case in point. Considering that long-term and large-scale mining is the main cause of ground subsidence in the mining area, countermeasures for ground subsidence damage can be implemented by adopting the following three main aspects. The first is the intensification of daily inspection of the surface structures and facilities and prompt reinforcement of damaged infrastructures to ensure normal operation and safety. The second is the reduction of the time spent in the mining and filling process, improvement

of the stiffness of the filling body, and reduction of the residual unfilled goaf to minimize the extent of surface subsidence and damage. The third is the conduct of rational planning for site selection of engineering facilities in the future based on regular surface monitoring to minimize the occurrence of deformation and damage.

6. Conclusions

This study illustrated that serious ground subsidence also can be induced by the backfill mining method. Three different subsidence troughs were formed in the three mine fields, especially bottom uplift occurred in the mine No. 1 after transition from open pit to underground mining.

The ground subsidence increased significantly and the maximum cumulated vertical displacement had reached 1,720 mm since 2001. The ground subsidence showed good correlations with the damage of underground facilities and the increase of the extracted ore tonnage.

Thus, continuous monitoring, as well as rational design of engineering works, can greatly help disaster prevention and control.

Acknowledgements

The research was supported by the National Natural Science Foundation of China (Grant Nos. 41002107, 40972197, 41172271, and 41030750) and the important direction project of Chinese Academy of Sciences knowledge innovation project (KZCX2-YW-Q03-02). Grateful appreciation is expressed for these supports.

References

Baldi P., Casula G., Cenni N., Loddo F., Pesci A., (2009), GPS-based monitoring of land subsidence in the Po Plain (Northern Italy), *Earth and Planetary Science Letters*, **288**, 204-212.

Bell F.G., Stacey T.R., Genske D.D., (2000), Mining subsidence and its effect on the environment: some differing examples, *Environmental Geology*, **40**, 135-152.

Carnec C., Delacourt C., (2000), Three years of mining subsidence monitored by SAR interferometry, near Gardanne, France, *Journal of Applied Geophysics*, **43**, 43-54.

Chrzanowski A., Szostak-Chrzanowski A., Bastin G., Lutes J., (2000), Monitoring and modelling of ground subsidence in mining areas: Case studies, *Geomatica*, **54**, 495-413.

Chrzanowski A., Chen Y.Q., Leeman R., Leal J., (1989), Integration of the Global Positioning System with Geodetic Leveling Surveys in Ground Subsidence Studies, *CISM Journal*, **43**, 377-386.

Cowling R., (1998), *Twenty-Five Years of Mine Filling: Development and Directions*, Proc. 6th Int. Symp. on Mining with Backfill, Brisbane, Australia, 3-10.

Cui X.M., Wang J.C., Liu Y.S., (2001), Prediction of progressive surface subsidence above longwall coal mining using a time function, *International Journal of Rock Mechanics and Mining Sciences*, **38**, 1057-1063.

Donovan J.G., Karfakis M.G., (2001), *The Effects of Backfilling on Ground Control and Recovery in Thin-Seam Coal Mining*, Proc. 7th Int. Symp. on Mining

with Backfill. The Society for Mining, Metallurgy, and Exploration, Inc. (SME), Littleton, CO, USA, 195-205.

González-Nicieza C., Álvarez-Fernández M.I., Menéndez-Díaz A., Álvarez-Vigil A.E., (2005), The new three-dimensional subsidence influence function denoted by n-k-g, *International Journal of Rock Mechanics and Mining Sciences*, **42**, 372-387.

Guéguen Y., Deffontaines B., Fruneau B., Al Heib M., de Michele M., Raucoules D., Guise Y., Planchenault J., (2009), Monitoring residual mining subsidence of Nord/Pas-de-Calais coal basin from differential and Persistent Scatterer Interferometry (Northern France), *Journal of Applied Geophysics*, **69**, 24-34.

Liu T.Y., Zhou C.P., Cai S.J., (1998), *New Development of Cemented Fill in Various Chinese Metal Mines*, Proc. 6th Int. Symp. on Mining with Backfill, Brisbane, Australia, 49-51.

Lü W.C., Cheng S.G., Yang H.S., Liu D.P., (2008), Application of GPS technology to build a mine subsidence observation station, *Journal of China University of Mining and Technology*, **18**, 377-380.

Oyler D.C., Mark C., Dolinar D.R., Frith R.C., (2001), A study of the ground control effect of mining longwall faces into open or backfilled entries, *Geotechnical and Geological Engineering*, **19**, 137-168.

Peng S.S.(Eds), 1992, *Third Workshop on Surface Subsidence Due to Underground Mining*, Proc. 3rd Workshop on Surface Subsidence Due to Underground Mining, West Virginia University, Morgantown, WV, 1-9.

Peyret M., Djamour Y., Rizza M., Ritz J.F., Hurtrez J.E., Goudarzi M.A., Nankali H., Chéry J., Le Dortz K., Uri F., (2008), Monitoring of the large slow Kahrod landslide in Alborz mountain range (Iran) by GPS and SAR interferometry, *Engineering Geology*, **100**, 131-141.

Sheorey P.R., Loui J.P., Singh K.B., Singh S.K., (2000), Ground subsidence observations and a modified influence function method for complete subsidence prediction, *International Journal of Rock Mechanics and Mining Sciences*, **37**, 801-818.

Shi C., Lou Y., Zhang H., Zhao Q., Geng J., Wang R., Fang R., Liu J., (2010), Seismic deformation of the Mw 8.0 Wenchuan earthquake from high-rate GPS observations, *Advances in Space Research*, **46**, 228-235.

Shimizu N., Tayama S., Hirano H., Iwasaki T., (2006), Monitoring the ground stability of highway tunnels constructed in a landslide area using a web-based GPS displacement monitoring system, *Tunnelling and Underground Space Technology*, **21**, 266-267.

Singh B., Saxena N.C.E. (Eds), 1991, *Land Subsidence*, Int. Symp., 11-15 Dec. 1989, Balkema A.A., Rotterdam, 51-66.

Singh K.B., Singh T.N., (1998), Ground movements over longwall workings in the Kamptee coalfield, India, *Engineering Geology*, **50**, 125-139.

Swift G.M., Reddish D.J., (2002), Stability problems associated with an abandoned ironstone mine, *Bulletin of Engineering Geology and the Environment*, **61**, 227-239.

Yamaguchi U., Yamatomi J., (1985), *Consideration on the effect of backfill for the ground stability*, Int. Symp. on Mining with Backfill, Lulea, Balkema A.A., Rotterdam, 443-451.